Article

The Tunnel of Acetyl-Coenzyme A Synthase/Carbon Monoxide Dehydrogenase Regulates Delivery of CO to the Active Site

Xiangshi Tan, Huay-Keng Loke, Shawn Fitch, and Paul A. Lindahl

J. Am. Chem. Soc., **2005**, 127 (16), 5833-5839• DOI: 10.1021/ja043701v • Publication Date (Web): 29 March 2005

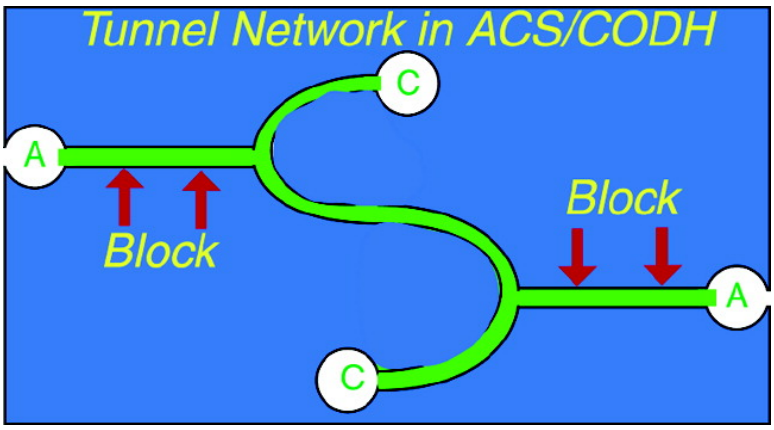

More About This Article

Additional resources and features associated with this article are available within the HTML version:

- Supporting Information
- Links to the 5 articles that cite this article, as of the time of this article download
- Access to high resolution figures
- Links to articles and content related to this article
- Copyright permission to reproduce figures and/or text from this article

View the Full Text HTML

Journal of the American Chemical Society is published by the American Chemical Society. 1155 Sixteenth Street N.W., Washington, DC 20036

J|A|C|S
ARTICLES
Published on Web 03/29/2005

The Tunnel of Acetyl-Coenzyme A Synthase/Carbon Monoxide Dehydrogenase Regulates Delivery of CO to the Active Site

Xiangshi Tan,[†] Huay-Keng Loke,[†] Shawn Fitch,[†] and Paul A. Lindahl*[,†,‡]

Contribution from the Departments of Chemistry and of Biochemistry and Biophysics, Texas A&M University, College Station, Texas 77843

Received October 16, 2004; E-mail: lindahl@mail.chem.tamu.edu

Abstract: The effect of [CO] on acetyl-CoA synthesis activity of the isolated α subunit of acetyl-coenzyme A synthase/carbon monoxide dehydrogenase from *Moorella thermoacetica* was determined. In contrast to the complete $\alpha_2\beta_2$ enzyme where multiple CO molecules exhibit strong cooperative inhibition, α was weakly inhibited, apparently by a single CO with $K_I = 1.5 \pm 0.5$ mM; other parameters include $k_{cat} = 11 \pm 1$ min^{-1} and $K_M = 30 \pm 10$ μM. The α subunit lacked the previously described "majority" activity of the complete enzyme but possessed its "residual" activity. The site affording cooperative inhibition may be absent or inoperative in isolated α subunits. Ni-activated α rapidly and reversibly accepted a methyl group from CH_3-Co^{3+}FeSP affording the equilibrium constant $K_{MT} = 10 \pm 4$, demonstrating the superior nucleophilicity of α_{red} relative to Co^{1+}FeSP. CO inhibited this reaction weakly ($K_I = 540 \pm 190$ μM). NiFeC EPR intensity of α developed in accordance with an apparent $K_d = 30$ μM, suggesting that the state exhibiting this signal is not responsible for inhibiting catalysis or methyl group transfer and that it may be a catalytic intermediate. At higher [CO], signal intensity declined slightly. Attenuation of catalysis, methyl group transfer, and the NiFeC signal might reflect the same weak CO binding process. Three mutant $\alpha_2\beta_2$ proteins designed to block the tunnel between the A- and C-clusters exhibited little/no activity with CO_2 as a substrate and no evidence of cooperative CO inhibition. This suggests that the tunnel was blocked by these mutations and that cooperative CO inhibition is related to tunnel operation. Numerous CO molecules might bind cooperatively to some region associated with the tunnel and institute a conformational change that abolishes the majority activity. Alternatively, crowding of CO in the tunnel may control flow through the tunnel and deliver CO to the A-cluster at the appropriate step of catalysis. Residual activity may involve CO from the solvent binding directly to the A-cluster.

Acetyl-coenzyme A synthase/carbon monoxide dehydrogenases are found in anaerobic archaea and bacteria that can grow chemo-autotrophically and play critical roles in C_1 metabolism.[1] The best-studied enzyme of this group is from the homoacetogen *Moorella thermoacetica* (previously *Clostridium thermoaceticum*).[2−8] This enzyme (ACS/CODH ≡ CODH/ACS) functions in the Wood/Ljungdahl autotrophic pathway by catalyzing reaction 1, the synthesis of acetyl-CoA from CO, CoA, and a methyl group donated from the corrinoid−iron−sulfur protein (CoFeSP).

$$CH_3-Co^{3+}FeSP + CO + CoASH \rightleftarrows CH_3(CO)SCoA + Co^{1+}FeSP + H^+ \quad (1)$$

$$Co^{1+}FeSP + CH_3-THF + H^+ \rightleftarrows CH_3-Co^{3+}FeSP + H-THF \quad (2)$$

$$CH_3-Co^{3+}FeSP + ACS/CODH_{red} \rightleftarrows CH_3-ACS/CODH_{ox} + Co^{1+}FeSP \quad (3)$$

$$CH_3-ACS/CODH_{ox} + CO \rightleftarrows CH_3(CO)-ACS/CODH_{ox} \quad (4)$$

$$CH_3(CO)-ACS/CODH_{ox} + CoASH \rightleftarrows CH_3(C)SCoA + ACS/CODH_{red} + H^+ \quad (5)$$

$$CO_2 + 2e^- + 2H^+ \rightleftarrows CO + H_2O \quad (6)$$

The methyl group originates from CH_3-THF (THF = tetrahydrofolate) and is transferred onto the reduced Co^{1+} state of CoFeSP in reaction 2, catalyzed by a methyltransferase (MT). The methyl group on CH_3-Co^{3+}FeSP can be transferred to the reduced form of ACS/CODH (reaction 3), leading to a stable methylated intermediate. Both methyl transfer steps occur by S_N2 mechanisms such that the stereochemical configuration of

[†] Department of Chemistry.
[‡] Department of Biochemistry and Biophysics.

(1) Wood, H. G.; Ljungdahl, L. G. *Variations in Autotrophic Life*; Academic Press: London, 1991; pp 201−250.
(2) Lindahl, P. A. *Biochemistry* **2002**, *41*, 2097−2105.
(3) Riordan, C. G. *J. Biol. Inorg. Chem.* **2004**, *9*, 509−510.
(4) Riordan, C. G. *J. Biol. Inorg. Chem.* **2004**, *9*, 542−549.
(5) Lindahl, P. A. *J. Biol. Inorg. Chem.* **2004**, *9*, 516−524.
(6) Brunold, T. C. *J. Biol. Inorg. Chem.* **2004**, *9*, 533−541.
(7) Volbeda, A.; Fontecilla-Camps, J. C. *J. Biol. Inorg. Chem.* **2004**, *9*, 525−532.
(8) Drennan, C. L.; Doukov, T. I.; Ragsdale, S. W. *J. Biol. Inorg. Chem.* **2004**, *9*, 511−515.

10.1021/ja043701v CCC: $30.25

the methyl group bound to THF is retained in acetyl-CoA.[9] This intermediate reacts with CO and CoASH to yield acetyl-CoA, probably by first reacting with CO to form an acetyl-intermediate (reaction 4) and then with CoA (reaction 5). Although CoA probably binds last, whether the methyl group or CO binds first is uncertain.

ACS/CODH is bifunctional and also catalyzes the reversible reduction of CO_2 to CO, reaction 6. The enzyme is an $\alpha_2\beta_2$ tetramer in which each β subunit contains the active site for CO/CO_2 redox catalysis, a novel [Ni Fe][Fe_3S_4] cluster called the C-cluster.[10−15] Each β subunit also contains an Fe_4S_4 cluster, while another such cluster bridges the two β subunits of an $\alpha_2\beta_2$ tetramer; these clusters are used to transfer electrons between the C-cluster and external redox agents. The α subunit contains the active site for acetyl-CoA synthesis, called the A-cluster. This cluster consists of a [Ni_pNi_d] dimer bridged to an Fe_4S_4.[13−15] Ni_p is thought to bind CO and accept the methyl group from CH_3-Co^{3+}FeSP. The A- and C-clusters are separated by ∼70 Å.

The ability of CO to serve as a substrate in the synthesis of acetyl-CoA has been recognized for 2 decades,[16] but only recently has CO_2 been recognized as a substrate (when a low-potential reductant such as methyl viologen or Ti citrate is included in the assay mix).[17] CO_2, or more technically an undifferentiated $\{CO_2/2e^-/2H^+\}$ unit, behaves as a classical Michaelis−Menten substrate. In contrast, CO is both a substrate and an inhibitor of catalysis.[18] Inhibition involves >2 CO's binding cooperatively and in an uncompetitive manner (i.e., to a form of the enzyme different from that to which substrate CO or CO_2 binds). Inhibition is incomplete, leaving a "residual" activity at 1 atm (980 μM) CO corresponding to about 10% of maximal (10% of 100 min^{-1} = 10 min^{-1}). Unlike the majority activity, this residual activity is not sensitive to cooperative CO inhibition.

The ability of either CO or CO_2 to be used as a substrate in acetyl-CoA synthesis raised the issue of whether the CO generated from CO_2 at the C-cluster migrates through solution to the A-cluster or travels to that cluster via a solvent-inaccessible pathway. The inability of hemoglobin (which binds CO rapidly and tightly) to attenuate acetyl-CoA synthesis when CO_2 was the substrate led to the proposal of a proteinaceous tunnel that connects the two active sites.[17] The X-ray crystal structure of the enzyme confirmed this, revealing an extensive tunnel network that connects not only the A- and C-clusters but the two C-clusters as well (Figure 1).[14,15]

The tunnel certainly channels CO from the site at which it is produced (i.e., the C-cluster) to the site at which it is consumed (the A-cluster), but the issue is undoubtedly more complex. The structure reported by Darnault et al. (2003) shows two conformations of the α subunits, called open and closed. The tunnel is blocked in the subunit with the open conformation but not in that with the closed conformation. This suggests that delivery of CO to the A-cluster is controlled by the conformation of α. Recently, we found that when Zn ions replace Ni_p, the enzyme is inactivated but only during catalysis.[20] This suggests that the conformation of α alternates during catalysis and that these conformational changes are vital to the catalytic mechanism, possibly by regulating delivery of CO to the A-cluster.

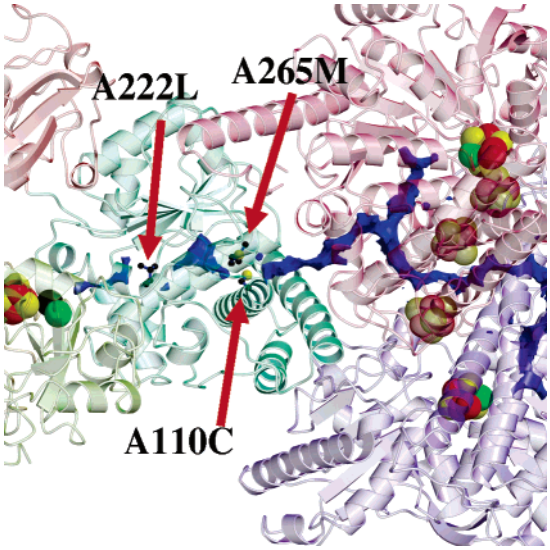

Figure 1. Structure of a portion of ACS/CODH emphasizing the location of mutations (arrows) and the tunnel (purple). The A-cluster is shown on the left, while the C, B′, D, B, and C′ clusters are shown on the right, from top to bottom.

The gene encoding the α subunit of ACS/CODH has been cloned and overexpressed in *Escherichia coli*.[21] The as-isolated recombinant subunit exhibits no catalytic activity (neither reaction 1 nor 6) but does exhibit acetyl-CoA activity after incubation in $NiCl_2$, as long as CO (rather than CO_2) is used as a substrate. Added Ni ions insert into the A-cluster to complete its assembly. The effect of [CO] on its activity has not been reported, and we wondered whether α would exhibit the same cooperative inhibition as ACS/CODH. In this paper, we describe those effects using the α subunit and three mutants of ACS/CODH designed to block the tunnel between the A- and C-clusters. Our results reveal that CO does not exhibit these inhibitory effects in α or in the mutants. These cooperative inhibitory effects of CO appear to involve the tunnel and to serve to regulate delivery of CO to the A-cluster during catalysis.

Experimental Procedures

Preparation of Proteins. Mutants A222L, A110C, and A265M (all located in the α subunit) were constructed as described[21,25] using plasmid pTM02 which contains the genes *acsA* and *acsB* as the

(9) (a) Lebertz, H.; Simon, H.; Courtney, L. F.; Benkovic, S. J.; Zydowsky, L. D.; Lee, K.; Floss, H. G. *J. Am. Chem. Soc.* **1987**, *109*, 3173−3174. (b) Tan, X.; Sewell, C.; Lindahl, P. A. *J. Am. Chem. Soc.* **2002**, *124*, 6277−6284.
(10) Dobbek, H.; Svetlitchnyi, V.; Gremer, L.; Huber, R.; Meyer, O. *Science* **2001**, *293*, 1281−1285.
(11) Drennan, C. L.; Heo, J.; Sintchak, M. D.; Schreiter, E.; Ludden, P. W. *Proc. Natl. Acad. Sci. U.S.A.* **2001**, *98*, 11973−11978.
(12) Feng, J.; Lindahl, P. A. *J. Am. Chem. Soc.* **2004**, *126*, 9094−9100.
(13) Dobbek, H.; Svetlitchnyi, V.; Liss, J.; Meyer, O. *J. Am. Chem. Soc.* **2004**, *126*, 5382−5387.
(14) Doukov, T. I.; Iverson, T. M.; Seravalli, J.; Ragsdale, S. W.; Drennan, C. L. *Science* **2002**, *298*, 567−572.
(15) Darnault, C.; Volbeda, A.; Kim, E. J.; Legrand, P.; Vernede, X.; Lindahl, P. A.; Fontecilla-Camps, J. C. *Nat. Struct. Biol.* **2003**, *10*, 271−279.
(16) Ragsdale, S. W.; Wood, H. G. *J. Biol. Chem.* **1985**, *260*, 3970−3977.
(17) Maynard, E. L.; Lindahl, P. A. *J. Am. Chem. Soc.* **1999**, *121*, 9221−9222.
(18) Maynard, E. L.; Sewell, C.; Lindahl, P. A. *J. Am. Chem. Soc.* **2001**, *123*, 4697−4703.
(19) Maynard, E. L.; Lindahl, P. A. *Biochemistry* **2001**, *40*, 13262−13267.
(20) Tan, X.; Bramlett, M. R.; Lindahl, P. A. *J. Am. Chem. Soc.* **2004**, *126*, 5954−5955.
(21) Loke, H.-K.; Tan, X.; Lindahl, P. A. *J. Am. Chem. Soc.* **2002**, *124*, 8667−8672.
(22) Lundie, L. L., Jr.; Drake, H. L. *J. Bacteriol.* **1984**, *159*, 700−703.
(23) Loke, H.-K.; Bennett, G. N.; Lindahl, P. A. *Proc. Natl. Acad. Sci. U.S.A.* **2000**, *97*, 12530−12535.
(24) Barondeau, D. P.; Lindahl, P. A. *J. Am. Chem. Soc.* **1997**, *119*, 3959−3970.

template, and the QuikChange site-directed mutagenesis method from Stratagene. Mutated genes were sequenced[23] to confirm that the desired mutations had been prepared. *M. thermoacetica* and recombinant *E. coli* cells were grown and harvested as described.[22,23] ACS/CODH, the α subunit, CoFeSP, and MT were purified as described[9,18,23] in a glovebox containing <1 ppm O_2. ACS/CODH proteins were isolated from mutant strains in a dithionite-reduced state, divided into aliquots, and frozen in liquid N_2. Protein concentrations were determined as described.[26] Each protein was >90% pure, as quantified by imaging Coomassie-Blue- (Bio-Rad) stained SDS-PAGE gels (Alpha Innotech Imager 2000). Portions were thawed as needed, subjected to a 1 cm × 20 cm column of Sephadex G25 equilibrated in Buffer A (50 mM Tris pH 8.0), divided into aliquots, and either used immediately or refrozen in liquid N_2. CO oxidation activity was measured as described.[27]

Methylation of CoFeSP and the α subunit of ACS/CODH. Ti^{3+}citrate was prepared from $TiCl_3$ (Aldrich) and standardized by titration against $K_3[Fe(CN)_6]$. Co^{1+}FeSP was methylated using CH_3-THF (Sigma) as described.[9,24] Analysis indicated 0.95 Co/$\alpha\beta$ for a CoFeSP sample and 0.99 Co/$\alpha\beta$ for a CH_3-Co^{3+}FeSP sample. The α subunit of ACS/CODH was activated with $NiCl_2$.[21] Samples were methylated by incubating with a 20-fold molar excess of Ti^{3+}citrate for 20 min, then adding CH_3-THF (5 molar equiv, relative to α), MT, and CoFeSP (1/20th molar equivalent, relative to α) and incubating overnight. The reaction was monitored spectrophotometrically at 390 nm. Resulting solutions were concentrated using a Centricon and subjected to Sephadex G25 chromatography to remove excessive Ti-citrate and CH_3-THF (neither MT nor CoFeSP would have been removed in this step). Acetyl-CoA synthase activity of the α subunit, wild-type ACS, and the three mutants were assayed as described.[18,21] X-band EPR spectra of ACS/CODH, the α subunit, and mutants were recorded at 130 or 10 K as described.[28]

Stopped-Flow Experiments. Pre-steady-state experiments were performed at 25 °C with an SF-61 DX2 double-mixing stopped-flow instrument (Hi-Tech Limited, UK) installed in an Ar-atmosphere glovebox (MJ Braun, Inc.) containing <1 ppm O_2.[9] Reactions were monitored in PM mode at 390 and 450 nm. Ar was passed through Oxysorb (MG Industries) filters, mixed with equivalently treated CO or CO_2 using a calibrated flow-meter (MG Industries, series 7941-AS2 4-tube), and passed into a reaction vessel containing protein solutions. Solutions were transferred to stopped-flow syringes by a custom-made cannula adapter as described.[9,18]

Kinetic Simulations. A computer program was used to simulate the Abs_{390} versus time and Abs_{450} versus time kinetic traces.[9] Simulations were quantitatively compared to experimental traces by calculating the sum of the squares of the residuals to obtain best-fit values. Best-fit concentrations were within ±0.5 μM of their experimentally determined values. Candidate extinction coefficients were ±~10% of their experimentally determined values. With improvements in fits, these limits were eventually set to ±<10%. Allowing these parameters to vary within the uncertainty of their experimentally determined values improved fits. For rate-constants, min/max limits were initially set liberally (from 10^{-4} to 10^{2}), but were gradually restricted as fits improved.

Indicated protein concentrations refer to final concentrations after mixing in the stopped-flow cell. The initial concentrations assumed for α were set at $^1/_3$ of those measured, so as to represent the concentration of functional Ni ions in the samples (the α subunit is heterogeneous such that only ~$^1/_3$ is catalytically functional). Experiments were performed using two independent batches of α, CoFeSP, and MT. Best-fit rate constants for data sets were averaged. Standard deviations for unknowns were determined by finding the value of that unknown required to increase residuals 1.5× while holding all other parameters fixed.

Results

Acetyl-CoA Synthase Activity of the α Subunit and the Effect of CO. Our initial objective was to determine the effect of CO on the ability of the Ni-activated α subunit to catalyze the synthesis of acetyl-CoA, and then to compare this effect to that observed using ACS/CODH. Initial rates (plotted as $v_{init}/[E_{tot}]$) increased with increasing [CO] in essentially hyperbolic fashion (Figure 2), maximizing at ~9 min^{-1} when [CO] was ~300 μM. Activity declined slightly thereafter, reaching 6 min^{-1} when [CO] = 980 μM (1 atm). This behavior indicates that CO is both a substrate and a weak inhibitor of acetyl-CoA synthesis.

A model was fitted to the data in an effort to extract kinetic constants. It assumed that substrate CO reversibly bound enzyme E, yielding a complex (ECO) that converted into E and product P (i.e., acetyl-CoA) in accordance with rate-constant k_{cat}. A single CO molecule was assumed to bind ECO with dissociation constant K_I, affording the nonproductive form $(CO)_1$ECO. The concentrations of all other components of the reaction were assumed to be invariant, as justified previously.[18] The best-fit to the data (Figure 2, dashed line) was acceptable, yielding $k_{cat} = 11 \pm 1$ min^{-1}, $K_M = 30 \pm 10$ μM, and $K_I = 1.5 \pm 0.5$ mM.

The methyl group transfer ability of Ni-activated α subunit was assessed using the stopped-flow kinetic method. CH_3-Co^{3+}-FeSP and Ti^{3+}citrate-reduced α_{red} were mixed, and the forward reaction was monitored at both 390 and 450 nm, wavelengths sensitive to an absorption feature of Co^{1+}FeSP. The reaction was rapid, approaching completion in ~0.5 s under all reaction conditions examined (Figure 3).

Concentrations of both CH_3-Co^{3+}FeSP and α_{red} were varied, as specified in Table 1. Reactions were performed in which CO was included in the CH_3-Co^{3+}FeSP syringe (Figure 3A), the α_{red} syringe (Figure 3B), and in both syringes (Table 1). The reverse reaction, in which CH_3-α_{ox} was mixed with Co^{1+}-FeSP, was also examined.

The model defined by reactions 7 and 8 fitted the data with acceptable fidelity. In the model, methyl group transfer is represented by a single step, and a single CO molecule is assumed to react with α_{red} to form an unmethylatable complex (α_{red}(CO)).

$$CH_3-Co^{3+}FeSP + \alpha_{red} \rightleftarrows CH_3-\alpha_{ox} + Co^{1+}FeSP \quad (7)$$

$$\alpha_{red} + CO \rightleftarrows \alpha_{red}(CO) \quad (8)$$

The same model fit all data sets and afforded a consistent set of rate constants (Table 1). Best-fit concentrations of α were 32% (±2%) of measured values, as expected for a heterogeneous population in which only that percentage have Ni_p in the proximal binding site of the A-cluster. The equilibrium constant for the methyl transfer reaction 7 was $K_{MT} = k_2/k_1 = (1.5 \pm 0.5\ \mu M^{-1}\ s^{-1})/(0.14 \pm 0.04\ \mu M^{-1}\ s^{-1}) = 10 \pm 4$. The dissociation constant for the CO binding reaction 8 was $K_{CO} = k_4/k_3 = (130 \pm 15\ s^{-1})/(0.24 \pm 0.08\ \mu M^{-1}\ s^{-1}) = 540 \pm 190$ μM.

As expected, EPR of the Ni-activated α subunit in the presence of 1 atm CO exhibited the NiFeC signal, with a spin intensity corresponding to 0.1−0.2 spins/α. The intensity of this signal was monitored as a function of [CO] and was found to

(25) Kim, E. J.; Feng, J.; Bramlett, M. R.; Lindahl, P. A. *Biochemistry* **2004**, *43*, 5725−5734.
(26) Pelley, J. W.; Garner, C. W.; Little, G. H. *Anal. Biochem.* **1978**, *86*, 341−343.
(27) Shin, W.; Lindahl, P. A. *Biochem. Biophys.* **1993**, *1161*, 379−396.
(28) Shin, W.; Lindahl, P. A. *J. Am. Chem. Soc.* **1992**, *114*, 9718−9719.

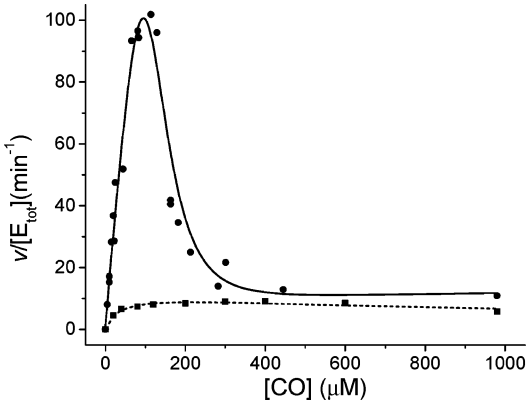

Figure 2. Initial rate of acetyl-CoA synthesis ($v/[E]_{tot}$) at increasing [CO] under an Ar atmosphere. α subunit (■, dashed line is best-fit simulation); native WT ACS/CODH from *M. thermoacetica* (●, solid line is best-fit simulation). Data and simulations of native WT ACS/CODH are adapted from ref 18.

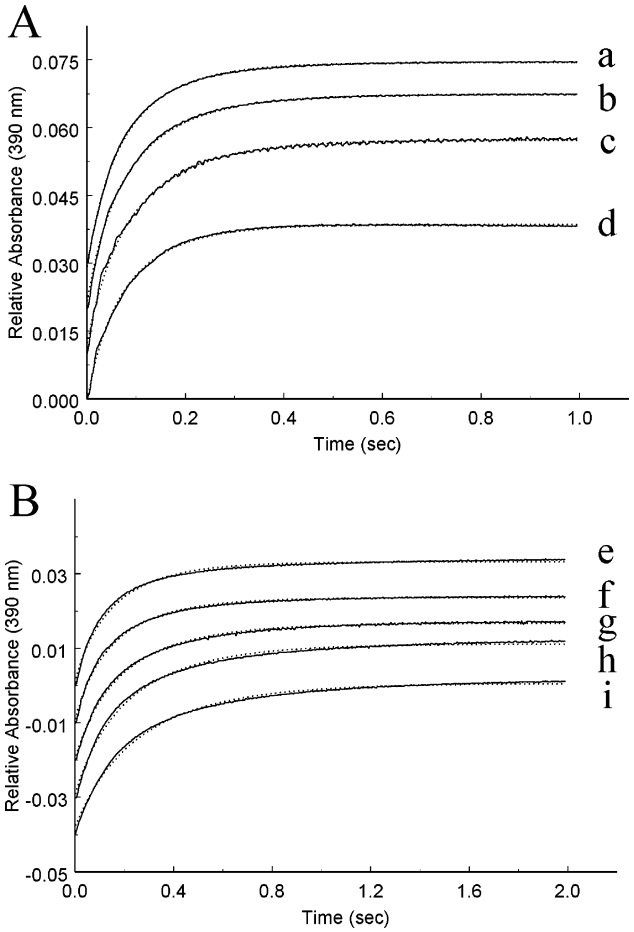

Figure 3. Stopped-flow reaction of CH_3Co^{3+}FeSP and the α subunit under different conditions and [CO]. (A) CH_3Co^{3+}FeSP was preincubated for 15 min in 50 mM Tris pH 8, 500 μM Ti^{3+}citrate at different concentrations of CO before mixing with the α subunit, which had been similarly preincubated with 500 μM Ti^{3+}citrate. (B) Same as (A) except CO was in the α syringe. Solid lines, experimental curves; dashed lines, best-fit simulations using reactions 7 and 8 and parameters in Table 1. Protein concentrations and simulations for a, b, c, d, e, f, g, h, and i correspond to experiments 9, 11, 13, 15, 19, 21, 23, 25, and 27 in Table 1, respectively.

develop in accordance with an apparent $K_d = 30$ μM (Figure 4).

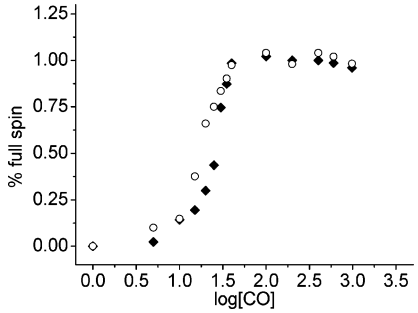

Figure 4. X-band EPR spectra of α subunit at 130 K (as a function of log[CO]): (○), α with 100 μM CoFeSP and 1 mM CoA; (◆), α only. Spectrometer conditions: microwave power, 80 mW; microwave frequency, 9.45 GHz; modulation frequency, 100 KHz; modulation amplitude, 11.8 G; center field, 3285 G; sweep width, 145 G; sweep time, 164 s; time constants, 328 s.

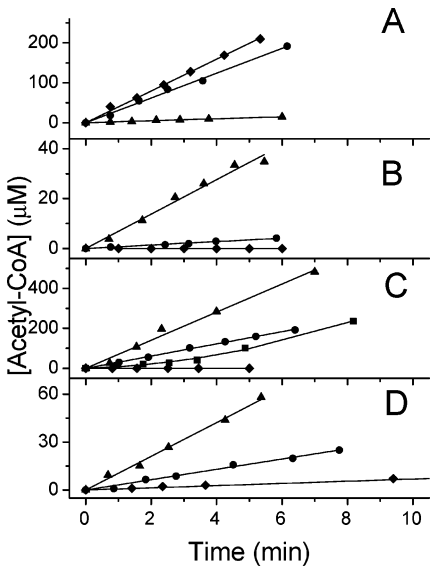

Figure 5. Acetyl-CoA synthase activity, performed as described[18] using CH_3THF, Coenzyme A, CoFeSP, MeTr, CO_2/CO in 50 mM MES buffer pH 6.3, 25 °C. (A) WT recombinant ACS/CODH in 1 atm CO_2 (◆), 100 μM CO (●), and 1 atm CO (▲). (B) Same as (A) except using A110C. (C) A222L in 1 atm CO_2 (◆), 1 atm CO (▲), and 100 μM CO, initiated by adding A222L and CoA (■) and by adding CoA alone, with A222L pre-added to the reaction mixture (●). (D) Same as (A) except using A265M.

Including CoA and CoFeSP in the α solution had little effect on the line shape of the titration curve or on the [CO] at which the signal developed. At [CO] > ∼200 μM, the intensity of the NiFeC signal declined slightly, possibly arising from the weak binding of CO to some site on the α subunit. An analogous phenomenon is not evident in plots of the NiFeC signal intensity versus [CO] for WT ACS/CODH; these simply plateau at high [CO].[29]

Acetyl-CoA synthase activity of recombinant ACS/CODH, expressed in *E. coli* and then activated with $NiCl_2$, was determined in assays containing 1 atm CO_2, 1 atm CO, and 100 μM CO. Initial rates normalized to total enzyme concentration were 20, 1.3, and 16 min^{-1}, respectively (Figure 5A).

These values are about 5× slower than for WT ACS/CODH biosynthesized in the native host *M. thermoacetica*. However, the qualitative behavior was the same, in that the rate in 1 atm CO is roughly 1/10th of that in 100 μM CO. This behavior

(29) Russell, W. K.; Lindahl, P. A. *Biochemistry* **1998**, *37*, 10016−10026.

Table 1. Methyl Transfer Reaction Parameters[a]

	exp.		best-fit		[CO]		$\mu M^{-1} s^{-1}$		s^{-1}		
exp. no.	μM MeCP	α	μM MeCP	$[Ni_p]$,[α-CO]	μM, in MeCP	α	k_1	k_2	k_3	k_4	λ_{max} nm
1	5	10	4.7	3.4			2.0	0.20			390
2	5	10	5.2	3.5			2.4	0.10			450
3	2.5	5	2.9	1.4			1.7	0.19			390
4	2.5	5	2.6	1.6			1.8	0.15			450
5	14	10	14.0	3.1			1.3	0.10			390
6	14	10	14.2	3.2			1.0	0.10			450
7	6	10	6.3	2.9			1.1	0.15			390
8	3	10	3.0	2.9			1.5	0.15			390
9	6	10	6.1	3.2	40	0	2.4	0.12			390
10	6	10	6.1	3.5	40	0	1.8	0.10			450
11	6	10	5.8	3.4	100	0	2.3	0.17			390
12	6	10	5.8	3.1	100	0	2.1	0.10			450
13	6	10	6.2	3.3	150	0	1.8	0.15			390
14	6	10	5.9	3.2	150	0	1.8	0.15			450
15	6	10	6.3	3.4	200	0	2.2	0.20			390
16	6	10	5.7	3.4	200	0	1.5	0.10			450
17	10	10	10.5	2.9	490	0	2.0	0.13			390
18	10	10	10.2	3.4	490	0	1.0	0.10			450
19	6	10	5.9	3.4	0	10	1.1	0.15	0.10	121	390
20	6	10	5.9	3.3	0	10	1.2	0.20	0.40	149	450
21	6	10	6.0	3.2	0	40	1.2	0.10	0.30	119	390
22	6	10	6.0	3.2	0	40	1.2	0.20	0.30	144	450
23	6	10	5.7	3.6	0	100	1.1	0.10	0.26	134	390
24	6	10	5.7	3.4	0	100	1.0	0.10	0.29	100	450
25	6	10	5.8	3.3	0	200	1.1	0.10	0.20	117	390
26	6	10	5.7	3.2	0	200	1.2	0.12	0.27	147	450
27	6	10	5.7	3.2	0	490	1.3	0.12	0.31	143	390
28	6	10	5.9	3.1	0	490	1.1	0.10	0.17	126	450
29	14	10	13.9	3.3	980	980	1.5	0.25	0.17	137	390
30	14	10	14.1	3.1	980	980	1.6	0.19	0.16	121	450
ave							1.5	0.14	0.24	130	
SD							0.5	0.04	0.08	15	
K_{fine}							1.5 ± 0.5	0.14 ± 0.04	0.24 ± 0.08	130 ± 15	

[a] Experiments 7 and 8 are for reverse reactions, and concentrations refer to $[Co^{+}FeSP]$ and $[CH_3$-α$]$, respectively. Experiments 1−18 used the first batch of proteins, while 19−30 used the second batch. k_1 and k_2 are the respective forward and reverse rate constants for reaction 7, while k_3 and k_4 are similarly defined for reaction 8. Best-fit $[Ni_p]$ refers to the concentration of α that contains Ni_p. Protein concentrations refer to after mixing in the stopped-flow cell. Extinction coefficients at 390 and 450 nm (in μM^{-1} cm^{-1}) for CH_3-Co^{3+}FeSP, Co^{1+}FeSP, α_{red}, and CH_3-α_{ox} are as reported.[32] For α_{red}-CO, extinction coefficients at 390 and 450 nm were measured to be 0.0078 and 0.0069, respectively. Best-fit values were 0.0084 ± 0.0006 and 0.0072 ± 0.0010, respectively.

indicates that the cooperative binding effect observed previously for native WT ACS/CODH is also present for recombinant WT enzyme. EPR spin intensity of NiFeC for this recombinant ACS/CODH was 0.12 spin/αβ. Activity levels and quantified NiFeC signal intensities vary somewhat between batches of recombinant ACS/CODH (more so than with native WT enzyme), probably due to differences in the extent of Ni-activation achieved.

Three mutant ACS/CODH proteins were prepared, including A110C, A222L, and A265M. In each case, altered residues were located in the α subunit at different locations within the tunnel region. The objective was to block the tunnel between the A- and C-clusters (illustrated in Figure 1) and to examine the effect of this on activity. Purified mutants were brown in color and exhibited EPR signals typical of WT ACS/CODH, including the NiFeC signal, the $g_{av} = 1.82$ and 1.86 signals (from the C_{red1} and C_{red2} states of the C-cluster), and the $g_{av} = 1.94$ signal (from the B_{red} state of the B-cluster) (Figure 6).

EPR spin intensity values of NiFeC of the Ni-activated A110C, A222L, and A265M in the presence of 1 atm CO were 0.17, 0.27, and 0.19 spin/αβ, respectively. The three mutants exhibited CODH activities of 280 (A110C), 300 (A222L), and 100 (A265M) μmol min^{-1} mg^{-1}, respectively, values similar to that obtained using recombinant WT ACS/CODH (200 μmol min^{-1} mg^{-1}). These characteristics indicate that the mutants folded properly and contained properly assembled metal centers, including the C-cluster.

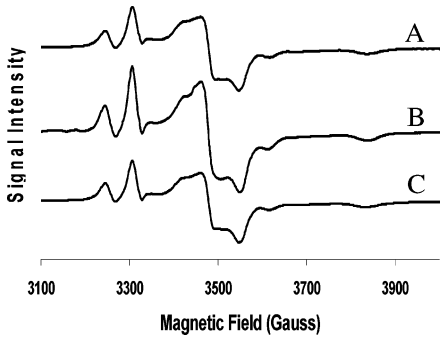

Figure 6. X-band EPR spectra of mutants of A110C (A), A222L (B), and A265M (C) at 10 K. Spectrometer conditions: microwave power, 20 mW; microwave frequency, 9.45 GHz; modulation frequency, 100 KHz; modulation amplitude, 11.8 G; sweep time, 167 s; time constants, 328 s.

Acetyl-CoA synthase activities were determined under the same conditions as above, in 1 atm CO_2, 1 atm CO, and 100 μM CO. A222L exhibited respective activities of 0, 35, and 15 min^{-1} (Figure 5C). The inability of A222L to synthesize acetyl-CoA using CO_2 as a substrate, despite a proper functioning C-cluster, is evidence that the tunnel connecting the C- and A-clusters was indeed blocked. The higher activity exhibited at 1 atm CO relative to 100 μM [CO] is distinctly different from native and recombinant WT ACS/CODH and is similar to that observed with the α subunit. Importantly, there is no

strong cooperative inhibition by CO. A222L exhibited a lag phase that could be eliminated by prereducing it in the assay mix (containing both CO and Ti^{3+}citrate) and by starting the reaction with CoA. This effect was unique to this mutant and suggests that the mutation somehow attenuated the rate at which the enzyme is reductively activated either by CO or by Ti^{3+}-citrate.

Mutant A110C exhibited respective activities of 0, 3.5, and 0.4 min^{-1} (Figure 5B), while A265M exhibited respective activities of 0.4, 5.3, and 1.6 min^{-1} (Figure 5D). The absence (or near absence) of activity using CO_2 as a substrate suggests that the tunnel was also blocked in these two mutations. The minor activity of A265M suggests that the tunnel was not completely blocked in it and that some CO molecules can still migrate to the A-cluster through the tunnel. Activities using CO as a substrate are qualitatively similar to but reduced relative to those of A222L, suggesting that the mutations involved in these two proteins had more complex effects than that in A222L (and that one of these effects caused activities with CO to decline). However, the most important result for these two mutants is the absence of strong cooperative inhibition of CO, which characterizes WT ACS/CODH. This demonstrates a correlation between a functional tunnel and this unusual form of inhibition.

Discussion

Comparing the data and simulation of Figure 2 for the α subunit (■ and dashed line) to those obtained using native WT ACS/CODH (● and solid line) suggests that the α subunit lacks the majority activity of ACS/CODH and possesses only the residual activity. This conclusion is supported by two pieces of evidence. First, the maximal initial rate obtained with α (10 min^{-1}) is 10-fold smaller than that obtained for native WT ACS/CODH (100 min^{-1}) and is similar to that obtained for the residual activity ($k_{res} = 10 \pm 5$ min^{-1}). Second, CO does not inhibit α strongly or in a cooperative manner. This is similar to the effect of CO on the residual activity in WT ACS/CODH but is different from the effect of CO on the majority activity. CO did inhibit the activity of α, but the effect was much weaker and noncooperative. The certainty of this conclusion is tempered by the low activity of recombinant WT ACS/CODH (20 min^{-1}), which we had hoped would have been about the same as native WT ACS/CODH. There are variations in the extent of Ni-activation with each preparation of the recombinant enzyme, and this may be the reason for the low activity. Another disparity is that the K_M for CO with α is ∼10× smaller than that estimated from the residual activity ($K_{M-res} = 200 \pm 100$ μM);[18] however, the uncertainty associated with the latter number might be greater than previously estimated, because the fits used to generate it involved ∼10 unknown parameters. Overall, the evidence qualitatively favors the conclusion that the isolated α subunit exhibits only the residual activity of WT ACS/CODH.

The three tunnel mutants are more similar to the α subunit than to native or recombinant ACS/CODH in that they do not display strong cooperative inhibition by CO. This suggests that the tunnel region of the enzyme (which is partially absent in the isolated α subunit and probably blocked in the mutants) is associated with cooperative CO inhibition and the majority activity. Interestingly, Seravalli et al. found that this cooperative CO inhibition is absent in one of the exchange reactions catalyzed by ACS/CODH, in which the carbonyl of acetyl-CoA exchanges with free CO.[30] Our results suggest that the free CO that exchanges with the carbonyl in this reaction does not migrate through the tunnel, but binds the A-cluster directly from solvent.

This cooperative inhibition may control the flow of CO to the A-cluster and ensure delivery of a single CO at the appropriate step of catalysis. At sufficiently low [CO], there is no inhibition and a single CO would be delivered; at high [CO], multiple CO molecules would bind cooperatively and attenuate the flow of CO through the tunnel and to the A-cluster. In contrast, the residual activity appears to involve unregulated CO binding directly to the A-cluster from solvent. CO delivery to the A-cluster through the tunnel appears more efficient (higher k_{cat}, smaller K_M) than direct CO binding from solvent. Under in vivo conditions, we suspect that the tunnel funnels CO directly to the A-cluster, allowing reaction at rapid rates, while maintaining a low CO concentration in the cytoplasm (which may prevent disadvantageous binding of CO to other sites within the cell).

The site on the enzyme to which CO molecules bind and induce cooperative inhibition is uncertain, but it appears to be located in the β subunit and to be structurally connected to the tunnel. One could imagine a conformational change caused by the binding of multiple CO's and serving to abolish flow through the tunnel. Given that the diameter of the tunnel is similar to that of CO in some regions, the conformational change required for this could be quite small and need not extend long distances from the binding site. CO-treated ACS/CODH exhibits numerous IR stretching frequencies in the region associated with terminally bound M−CO complexes.[31] One feature at 1996 cm^{-1} was shown to arise from CO bound to the A-cluster in the A_{red}-CO state, while others at 2074, 2044, 1970, 1959, and 1901 cm^{-1} probably reflect binding at the C-cluster. These stretching frequencies could reflect the binding of more than one CO to the C-cluster or a single CO bound to different C-cluster conformers. It is tempting to assume the former and associate such bindings to the cooperative CO-inhibition effect. However, CO oxidation activity is not inhibited by high [CO], leaving us with a complicated scenario in which the binding of multiple CO's to the C-cluster would inhibit flow through the tunnel but not affect CO oxidation activity.

Another scenario would have multiple CO's binding to other metal clusters in the β subunit, but this seems unlikely as no exogenous ligands are coordinated to these clusters in the X-ray crystal structure of the CO-treated enzyme, and these clusters seem to function simply in electron transfer processes. Another possibility is that the site for cooperative CO inhibition is not actually a distinct binding site, but the result of CO crowding within the tunnel. Due to the small diameter of the tunnel relative to the size of CO, the flow of CO might attenuate cooperatively when [CO] exceeds a critical value. Multiple CO molecules might interact with residues on the tunnel wall and block passage of other CO's through the tunnel. Although individual noncovalent molecular interactions would be undoubtedly weak,

(30) Seravalli, J.; Kumar, M.; Ragsdale, S. W. *Biochemistry* **2002**, *41*, 1807−1819.
(31) Chen, J. Y.; Huang, S.; Seravalli, J.; Gutzman, H.; Swartz, D. J.; Ragsdale, S. W.; Bagley, K. A. *Biochemistry* **2003**, *42*, 14833−14830.
(32) Tan, X.; Sewell, C.; Yang, Q.; Lindahl, P. A. *J. Am. Chem. Soc.* **2003**, *125*, 318−319.

collectively they might suffice to cause the observed inhibition. These interactions have strong distance dependence such that their strength might become significant as the diameter of the tunnel narrows and a larger percentage of CO molecules interact with the walls of the tunnel. We are intrigued by this possibility but realize that it needs to be evaluated further before it should be viewed as anything more than speculation.

The methyl group transfer properties of the α subunit are similar to those of ACS/CODH, in that reaction 7 is reversible and favors formation of product. The calculated K_{eq} reveals the superior nucleophilicity of α_{red} relative to Co^{1+}FeSP, a well-known nucleophile. Comparing the rate and equilibrium constants quantitatively to ACS/CODH is difficult because the model used to fit the data of α required only the single reaction 7, while that for ACS/CODH required three steps, including the association of ACS/CODH and CH_3-Co^{3+}FeSP, methyl group transfer, and the dissociation of CH_3-ACS/CODH and Co^{1+}FeSP.[9]

The EPR experiments presented here and involving α suggest that the CO which binds to Ni_p in forming the A_{red}-CO state and the associated NiFeC signal does not inhibit catalysis or methyl group transfer. We conclude this because the K_d associated with this binding (~30 μM) is more than an order of magnitude smaller than that involved in inhibiting catalysis (K_I = 1.5 mM) and methyl group transfer (K_{CO} = 540 μM). This is contrary to an earlier conclusion from our group that this state inhibits catalysis.[19,24] This difference between K_d and K_I, and the similarity between K_d and K_M for CO measured here for the α subunit (both ~30 μM), supports the conclusion of Ragsdale that the A_{red}-CO state is an intermediate of catalysis.[30] It also supports a Ni_p^{1+}-based mechanism of catalysis, although other results favor a Ni_p^0-based mechanism.[5] Further studies will be required to settle these mechanistic issues.

The fact that CO weakly inhibits catalysis, methyl group transfer, and possibly attenuates the NiFeC signal suggests that the three phenomena might reflect the same binding event, that of a single CO to some site on the α subunit. The respective dissociation constants for the processes are not identical (K_I = 1.5 mM and K_{CO} = 540 μM), but they are all weak and thus notoriously difficult to measure. Presumably, there would be an analogous binding site for a single CO in ACS/CODH. CO does inhibit methyl group transfer of ACS/CODH (with K_I = 190 μM), and the model assuming the binding of a single CO fit these data as well as those assuming multiple CO's. The effect of CO on the catalytic activity of ACS/CODH is dominated by the CO-cooperative binding event, which might obscure a weaker noncooperative CO binding event.

Volbeda and Fontecilla-Camps have raised the critical issue of where CO_2 and CO enter/exit ACS/CODH when these molecules oxidize and reduce, respectively, at the C-cluster and/or become incorporated into acetyl-CoA at the A-cluster.[7] Maynard and Lindahl found that CO does not "leak" from the tunnel when ACS/CODH operates in acetyl-CoA synthesis, implying that the exit port for CO is gated in a manner sensitive to the synthase reaction.[19] According to the X-ray structures, the only ports of the tunnel appear to be at the two environment: A-cluster interfaces in the $\alpha_2\beta_2$ tetramer, with access controlled by the conformation of α. One possibility is that the CO_2 used in acetyl-CoA synthesis enters the enzyme through the port with the α subunit permanently in the closed conformation (i.e., with Zn or Cu in the proximal site of the A-cluster). Assuming that the mutations designed to block the tunnel in the region between the A- and C-clusters are indeed blocked in this manner, the substantial CO oxidation activity of these mutants falsifies this possibility and suggests that another pathway (not identified in the crystal structures) connects the C-cluster to the environment. This hypothetical pathway would allow CO_2 or CO to enter the protein, migrate to the C-cluster, and eventually migrate to the A-cluster for incorporation into acetyl-CoA. The nonleakiness of the tunnel toward CO while the enzyme is in synthase mode[19] suggests that this hypothetical entry port would not be an exit port for CO during the synthesis of acetyl-CoA. Additional studies are required to further evaluate the entry and exit ports for CO and CO_2 as well as the overall function of the tunnel in ACS/CODH.

Acknowledgment. This work was supported by the National Institutes of Health (GM46441). We thank Anne Volbedaand and Juan C. Fontecilla-Camps (Institut de Biologie Structurale, Grenoble France) for suggesting which residues of the tunnel region should be mutated, for preparing Figure 1, and for helpful critical discussion. We also thank Ivan V. Surovtsev for fitting the data of Figure 2. The National Institutes of Health (GM46441) sponsored this study.

JA043701V